

Experimental Simulation of Bosonic Creation and Annihilation Operators in a Quantum Processor

Xiangyu Kong,^{1,*} Shijie Wei,^{2,*} Jingwei Wen,¹ and Gui-Lu Long^{1,3,4,†}

¹*State Key Laboratory of Low-Dimensional Quantum Physics and Department of Physics, Tsinghua University, Beijing 100084, China*
²*IBM Research, China*

³*Tsinghua National Laboratory for Information Science and Technology, Beijing 100084, P. R. China.*

⁴*Collaborative Innovation Center of Quantum Matter, Beijing 100084, China*

(Dated: July 12, 2021)

The ability of implementing quantum operations plays fundamental role in manipulating quantum systems. Creation and annihilation operators which transform a quantum state to another by adding or subtracting a particle are crucial of constructing quantum description of many body quantum theory and quantum field theory. Here we present a quantum algorithm to perform them by the linear combination of unitary operations associated with a two-qubit ancillary system. Our method can realize creation and annihilation operators simultaneously in the subspace of the whole system. A prototypical experiment was performed with a 4-qubit Nuclear Magnetic Resonance processor, demonstrating the algorithm via full state tomography. The creation and annihilation operators are realized with a fidelity all above 96% and a probability about 50%. Moreover, our method can be employed to quantum random walk in an arbitrary initial state. With the prosperous development of quantum computing, our work provides a quantum control technology to implement non-unitary evolution in near-term quantum computer.

PACS numbers: 03.67.Ac, 03.67.Lx, 42.50.Pq, 85.25.Cp

I. INTRODUCTION

The non-Hermitian bosonic operators \hat{a} and \hat{a}^\dagger introduced in harmonic oscillator question is a basic and crucial concept in quantum mechanics, laying the foundation for quadratic quantization[1]. They offer us an alternative way to calculate harmonic oscillator system without solving the irksome differential equations[2, 3]. These bosonic operators also play an important role in many fields of physics such as quantum optics[4], quantum mechanics[1, 5], quantum measurement[6] and even quantum chemistry[7]. According to existing research, the annihilation and creation operation can be foundations to construct arbitrary quantum state in theory[8]. Considering the hot field of quantum computation and quantum information, it is natural to for us try to realize these operators in steerable quantum system which can provide us a novel way to design quantum algorithm. The designed quantum system is difficult to execute non-unitary operator, which means there will be an obstacle to evolve the max and min quantum state to zero state in the process of realizing creation and annihilation operators. Given the importance of these operators, efficiently performing them with high success probability and fidelity in quantum process is critical. Recently, we realize some experiment progress and some works focus on realizing the bosonic operations at the single-boson level in optical system[4]. But the probability of success and performance fidelity are things belong to coin's different sides in general. Some improvements have been done in trapped ion system realizing deterministic addition and near-deterministic subtraction of bosonic particle with fidelity over

0.9[9]. However, improvements still need to be made to satisfy higher precision and less experiment times demanded.

In this paper, we experimentally realize creation and annihilation operators using the combination of unitary operators in a four-qubit nuclear magnetic resonance (NMR) system for the first time. The results offer us a raise both in experiment precision and success ratio. The paper is organized as follows: In Sec. II, we introduce the universal theory of how to realize these two non-unitary operators. In Sec. III, we take the four-qubit sample as an example to introduce our experimental setups and experimental procedure. Then, we present the experimental results and discuss the consequences. In Sec. IV, we report an application of our algorithm. At last, we close with a conclusion section summarizing the entire work and giving some prospects.

II. THEORY

Quantum mechanically, creation \hat{a}^\dagger and annihilation \hat{a} operators acting on a bosonic system with number N of identical particles satisfy the following operator relationship[10]:

$$\begin{aligned}\hat{a}^\dagger|N\rangle &= \sqrt{N+1}|N+1\rangle \\ \hat{a}|N\rangle &= \sqrt{N}|N-1\rangle.\end{aligned}\tag{1}$$

Given the importance of the creation and annihilation operators, efficiently performing them in a quantum process is critical. However, implementing such bosonic operations is challenging. Because the fact that these operators are non-unitary and inherently probabilistic, cannot be realized during the Hamiltonian evolution of a physical system without enlarging the Hilbert space.

Ignoring the modification of the probability amplitude of state, the conventional addition and subtraction of a particle

* These two authors contribute equally to this study.

† Correspondence and requests for materials should be addressed to G.L.L.:gllong@tsinghua.edu.cn

can be expressed as

$$\begin{aligned}\hat{K}^\dagger|N\rangle &= |N+1\rangle \\ \hat{K}|N\rangle &= |N-1\rangle.\end{aligned}\quad (2)$$

which can be called addition and subtraction operation.

We consider addition and subtraction operators with identical particles number N . Our method can realize addition \hat{K}^\dagger and subtraction \hat{K} operators in one quantum circuit.

In our method, the identical particles number N is mapped to a corresponding $|N\rangle$ state. For convenience, we adopt a truncated form of creation operation \hat{K}^\dagger by defining it as a $(N+1) \otimes (N+1)$ matrix

$$\hat{K}^\dagger = \sum_{i=0}^{N-1} |i+1\rangle\langle i|, \quad \hat{K} = \sum_{i=1}^N |i-1\rangle\langle i| \quad (3)$$

Every operation above can be decomposed into a sum form of two unitary operations.

$$\hat{K}^\dagger = \frac{U_0 + U_1}{2}, \quad \hat{K} = \frac{U_2 + U_3}{2}, \quad (4)$$

where

$$\begin{aligned}U_0 &= \sum_{i=0}^{N-1} |i+1\rangle\langle i| + |0\rangle\langle N| \\ U_1 &= \sum_{i=0}^{N-1} |i+1\rangle\langle i| - |0\rangle\langle N| \\ U_2 &= \sum_{i=1}^N |i-1\rangle\langle i| + |N\rangle\langle 0| \\ U_3 &= \sum_{i=1}^N |i-1\rangle\langle i| - |N\rangle\langle 0|.\end{aligned}$$

Considering the fact \hat{K}^\dagger and \hat{K} can be expressed into a linear combination of unitary operators, we can perform the addition and subtraction operators via duality quantum computing[11–14]. In duality quantum computing, the work system with initial state $|\Psi\rangle$ and the d -dimension ancillary system with initial state $|0\rangle$ are coupled together. The corresponding digital simulation quantum circuit of the addition and subtraction operators by the algorithm is further shown in Fig. 1.

As shown in Fig. 1, the unitary operators V and W performed on the two-qubit ancillary system are

$$V = H \otimes H \quad (5)$$

$$W = I \otimes H, \quad (6)$$

The circuit realizes the process:

$$\begin{aligned}|0\rangle_2|\Psi\rangle &\rightarrow \sqrt{\frac{1}{2}}\hat{K}^\dagger|00\rangle_2|\Psi\rangle + \sqrt{\frac{1}{2}}\hat{K}|10\rangle_2|\Psi\rangle \\ &+ \sqrt{\frac{1}{2}}\hat{J}^\dagger|01\rangle_2|\Psi\rangle + \sqrt{\frac{1}{2}}\hat{J}|11\rangle_2|\Psi\rangle.\end{aligned}\quad (7)$$

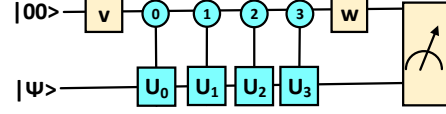


Figure 1. Quantum circuit of realizing addition and subtraction operators. $|\Psi\rangle$ denotes the initial state of work system, and $|00\rangle$ is the initial state of auxiliary system. The squares represent unitary operations and the circles represent the state of the controlling qubit. Unitary operations U_0 , U_1 , U_2 and U_3 are activated only when the auxiliary qubit is $|00\rangle$, $|01\rangle$, $|10\rangle$ and $|11\rangle$ respectively. We "readout" two outputs with the first auxiliary system in state $|00\rangle$, $|10\rangle$.

where the operators \hat{K}^\dagger , \hat{K} , \hat{J}^\dagger , \hat{J} are acting on the work system $|\Psi\rangle$. To be the same with \hat{K}^\dagger and \hat{K} in the Eq. 7, the operators \hat{J}^\dagger and \hat{J} can be calculated by

$$\hat{J}^\dagger = \frac{U_0 - U_1}{2} = |0\rangle\langle N|, \quad \hat{J} = \frac{U_2 - U_3}{2} = |N\rangle\langle 0|. \quad (8)$$

The \hat{J}^\dagger operation transform $|N\rangle$ state into $|0\rangle$ state, and \hat{J} transform $|0\rangle$ state into $|N\rangle$ state. So it is clear that the operator \hat{J}^\dagger is a special addition operator dealing with the maximum state and the operator \hat{J} is the special subtraction operator dealing with the minimum state. The probability of realization of addition operator and subtraction are both 50%.

Then we will consider addition and subtraction operations in the case where identical particles number $N = 3$ in Eq. 4.

III. EXPERIMENT AND RESULT

We experimentally inspect our algorithm using four-qubit nuclear magnetic resonance (NMR) system. As introduce before, the ancillary system is two qubits and we choose a two-qubit work system $|00\rangle$, $|01\rangle$, $|10\rangle$, $|11\rangle$ to represent 0,1,2,3. The four-qubit sample is ^{13}C -labeled trans-crotonic acid dissolved in d6-acetone. The structure of the molecule is shown in Fig. 3, where C_1 to C_4 denote the four qubits, the first two qubits are auxiliary system and the last two qubits are the work system. The methyl group M , H_1 and H_2 were decoupled throughout all experiments. For molecules in liquid solution, both intramolecular dipolar couplings (between spins in the same molecule) and intermolecular dipolar couplings (between spins in different molecules) are averaged away by the rapid tumbling[15]. The internal Hamiltonian under weak coupling approximation is

$$\mathcal{H} = - \sum_{j=1}^4 \frac{1}{2} \omega_j \sigma_z^j + \sum_{j < k}^4 \frac{\pi}{2} J_{jk} \sigma_z^j \sigma_z^k, \quad (9)$$

where ν_j is the chemical shift and J_{jk} is the J-coupling strength. All experiments were carried out on a Bruker DRX 400MHz spectrometer at room temperature (296.5K).

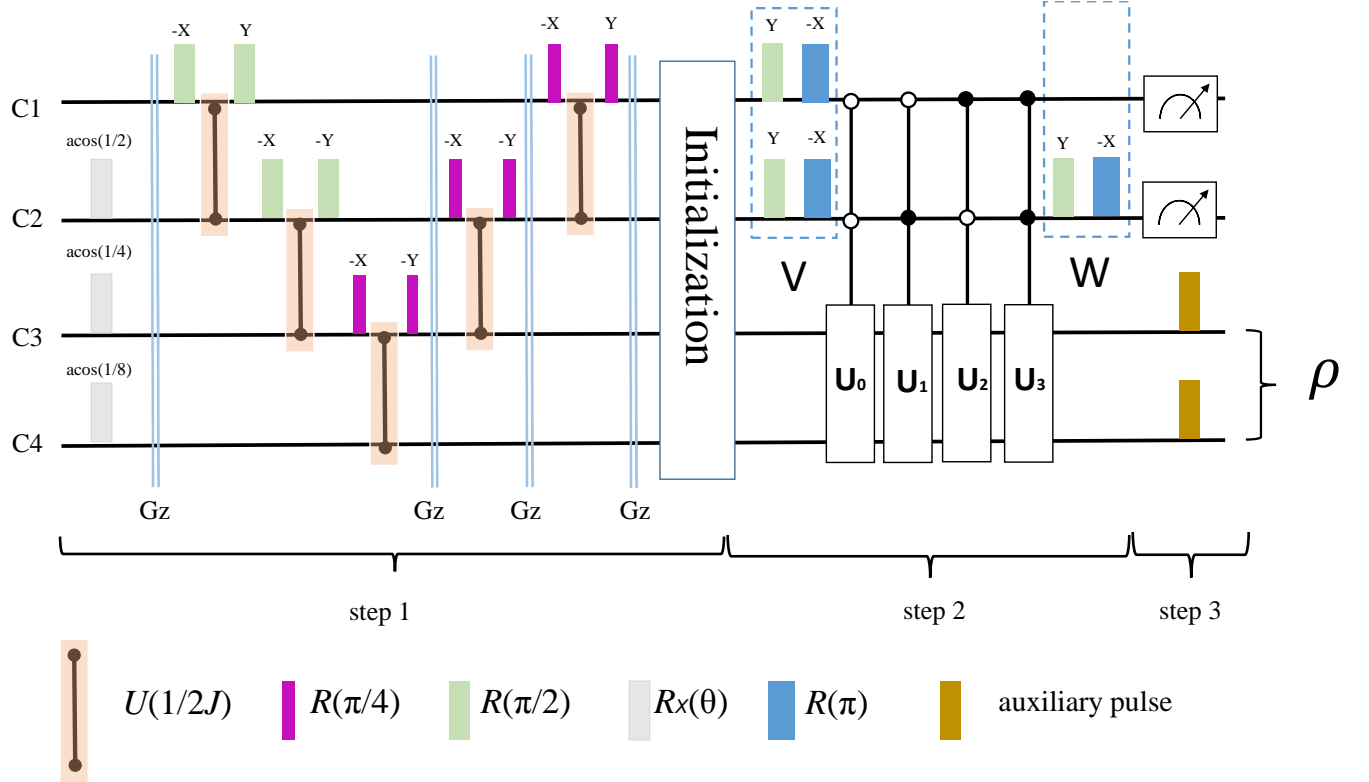


Figure 2. **NMR sequence to realize the addition and subtraction operators.** In the first step, we use spatial averaging method to prepare the pseudo-pure state. In this part, the purple rectangles stand for the unitary operations which rotate forty-five degrees with a coordinate axis. Similarly, the green rectangles rotate ninety degrees. The white rectangles stand for the unitary operations which rotate the special angle with X axis. The blue rectangles stand for the unitary operations which rotate one hundred and eighty degrees with Y axis. The double straight lines stand for the gradient field in the z direction. In the second step, the radio-frequency (RF) pulses during this procedure are optimized by the GRAPE technology to realize the controlled operator. In the third step, we measure the first two qubits and use the quantum tomography technology to obtain the final density matrix. The brown squares are the auxiliary pulse which can be used for quantum tomography.

	C1	C2	C3	C4	
C1	1705.5				Crotonic Acid
C2	41.64	14558.0			
C3	1.46	69.72	12330.5		
C4	7.04	1.18	72.36	16764.0	
T2	0.84	0.92	0.66	0.79	

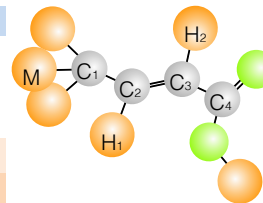


Figure 3. Molecular structure and Hamiltonian parameters of ^{13}C -labeled trans-crotonic acid. C_1 , C_2 , C_3 and C_4 are used as four qubits. The chemical shifts and J-couplings (in Hz) are listed by the diagonal and off-diagonal elements, respectively. T_2 (in Seconds) are also shown at bottom.

The entire experiment can be divided into three parts and its experimental circuits are shown in Fig. 2.

Step1:Initialization—Starting from thermal equilibrium state, we drive the system to the pseudo-pure state (PPS) with the method of the spatial averaging technique [16, 17, 19, 21]. Step 1 in Fig. 2 is the experimental circuit realizing PPS where all local operations are optimized using the gradient ascent pulse engineering(GRAPE) with a fidelity over 99.5%[22, 23]. The final form of four-qubit PPS is $\rho_{0000} =$

$(1 - \epsilon)\mathbb{I}/16 + \epsilon|0000\rangle\langle 0000|$, where \mathbb{I} is identity matrix and $\epsilon \approx 10^{-5}$ is the polarization. Since only the deviated part $|0000\rangle$ contributes to the NMR signals, the density matrix used in NMR are all deviated matrix and the PPS is able to serve as an initial state. The experimental results are represented as the density matrices obtained by the state tomography technique [24–26] shown in Fig. 4. The fidelity between the experimental results and $|0000\rangle$ is over 99.02%.

Step2:operator—As we introduced in the Sec. II, we perform the addition and subtraction operator \hat{K}^\dagger , \hat{K} by the duality quantum computing. In this case, $\text{C}1$ and $\text{C}2$ represent the ancillary system with initial state $|0\rangle$, $\text{C}3$ and $\text{C}4$ represent the work system as shown in Fig.2. The unitary operator V and W performed on the $\text{C}1$ and $\text{C}2$ can be realized as shown in step2 at Fig.2. Moreover, the four Control-U operators can be realized by using the GRAPE technology with a fidelity over 99.5%.

Step3:Mesurement— The measurement circuit is also listed in Fig. 2 at Step 3. From Eq. 7, we know that the operator applied on work system depends on the measurement of the ancillary system. So we have to measure the ancillary qubits and use quantum tomography technology to get the density

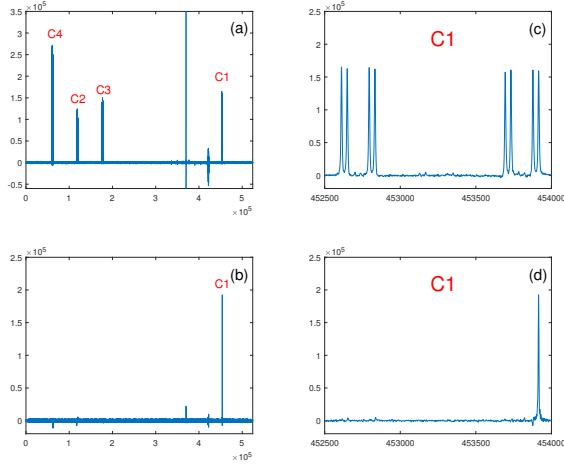


Figure 4. The spectrum of thermal equilibrium state and PPS. (a) The spectrum of the thermal equilibrium state. The x axis is the relative frequency and the y axis is the amplitude in arbitrary unit. Since the qubits are all carbon atoms, all signal of these four qubits can be detected through carbon channel in NMR experiments. (b) The spectrum of spin C1 in the thermal equilibrium state. This is an expanded view of spin C1 in (a). From this figure, we can observe more information in detail. Quantum state of remaining spins (C2, C3 and C4) is as indicated, based on J14, J24 and J34 shown in Fig. 3. (c) The spectrum of the PPS. As we know, the ground state $|0000\rangle$ can not be detected directly in NMR and we can apply the $R_y^i(\pi/2)$ on it to obtain a single peak of the i th spin. In our case, only the peak in the spectrum of C1 can be detected by applying $R_y^1(\pi/2)$ pulse. (d) The spectrum of spin C1 in PPS. This is also an expanded view of spin C1 in (c). It is clear that the peaks standing for the quantum state except $|0\rangle$ are close to zero.

matrix by applying auxiliary pulses on C3, C4.

IV. RESULT

Here we will introduce two examples in detail with two different initial quantum states to show our algorithm. One is general quantum state such as $|\phi\rangle = |01\rangle$, the other is superposition state such as $|\phi\rangle = \frac{|01\rangle + |10\rangle}{\sqrt{2}}$. These initial states can be obtained by single-qubit gates and C-NOT gate from the ground state $|00\rangle$. Then we can get the experimental results shown below by following the steps introduced above.

A. general state

The experimental results of the first example are shown in Fig. 6. We can find that the addition operation can be realized when the auxiliary qubits are $|00\rangle$. Then we calculate the fidelity by definition[27]:

$$F(\rho, \sigma) = |Tr(\rho\sigma)|/\sqrt{Tr(\rho^2)Tr(\sigma^2)} \quad (10)$$

where ρ and σ represents the density matrix getting from the experiments and theories respectively. So comparing the experiments shown in Fig. 5(b) with the quantum state $|10\rangle$, the

Table I. The measurement of the auxiliary qubit.

	$ 00\rangle$	$ 10\rangle$	$ 01\rangle$ and $ 11\rangle$
Parobability	49.56%	49.51%	0.93%

fidelity between them is over 98.8%. Thus we probabilistically realize the quantum process:

$$\hat{K}^\dagger |01\rangle = |10\rangle \quad (11)$$

Similarly, the subtraction operator can be performed when the auxiliary qubit is $|10\rangle$ shown in Eq. 8. Comparing the results shown Fig. 5 (c) with theoretical state $|00\rangle$, the fidelity between them is approximately equal to 98.3%. Thus we also probabilistically realize the quantum process:

$$\hat{K}|01\rangle = |00\rangle \quad (12)$$

We introduce that the addition and subtraction operators can be performed in probability. From the Eq. 8, the probabilities depends on the experimental results of the auxiliary qubit shown in Tab. II. The measurement of $|11\rangle$ should be an experimental error. From the results we can find that we can perform the addition and subtraction operator for the same probability 50%.

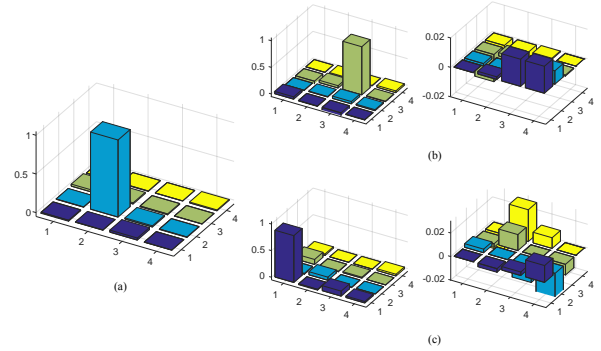


Figure 5. The density matrix of the initial quantum state and final state. (a) The initial quantum state $|01\rangle$. (b) The final state when the measurement of ancillary qubits is $|00\rangle$. (c) The final state when the measurement of ancillary qubits is $|10\rangle$. Moreover, the right part is the real part of the density matrix and the left part is the imaginary part in (b) and (c).

B. superposition state

The experimental results of the second example are shown in Fig. 6. Similarly, we can find that the addition operation can be realized when the auxiliary qubit is $|00\rangle$. Then we calculate the fidelity by the definition Eq. 13.

So comparing the experiments shown in Fig. 6 (b) with the quantum state $\frac{|01\rangle + |10\rangle}{\sqrt{2}}$, the fidelity between them is over

Table II. The measurement of the auxiliary qubit.

	$ 00\rangle$	$ 10\rangle$	$ 01\rangle$ and $ 11\rangle$
Parobability	48.84%	49.79%	1.38%

96.3%. Thus we realize the quantum process probabilistically:

$$K^+ \frac{|01\rangle + |10\rangle}{2} = \frac{|10\rangle + |11\rangle}{2} \quad (13)$$

Similarly, the subtraction operator can be performed when the auxiliary qubit is $|10\rangle$ shown in Eq. 8. Comparing the results shown Fig. 6(c) with theoretical state $\frac{|01\rangle + |10\rangle}{2}$, the fidelity between them is approximately equal to 97.0%. Thus we also realize the quantum process probabilistically:

$$K^- \frac{|01\rangle + |10\rangle}{2} = \frac{|00\rangle + |10\rangle}{2} \quad (14)$$

We introduce that the addition and subtraction operators can be performed in probability. From the Eq. 8, the probabilities depends on the experimental results of the auxiliary qubit shown in Tab. II. The measurement of $|11\rangle$ should be an experimental error. From the results we can find that we can perform the addition and subtraction operator for the same probability 50%.

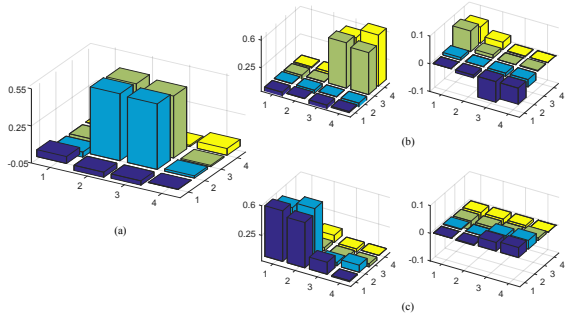


Figure 6. The density matrix of the initial quantum state and final state. (a) is the initial quantum state $\frac{|01\rangle + |10\rangle}{2}$. (b) is the final state when the measurement of ancillary qubits is $|00\rangle$. (c) is the final state when the measurement of ancillary qubits is $|10\rangle$. Moreover, the right part is the real part of the density matrix and the left part is the imaginary part in (b) and (c).

V. APPLICATION

We have presented a universal algorithm to preform addition and subtraction operator using a two-qubit auxiliary system above. Our algorithm has many applications and one of them is quantum random walks[28]. Quantum random walks (QRWs) are extensions of the classical counterparts and have wide applications in quantum algorithms[29], quantum simulation[30], quantum computation[31], and so on[32]. In standard one-dimensional (1D) discrete-time quantum walks(DTQWs), the walker's position can be denoted as

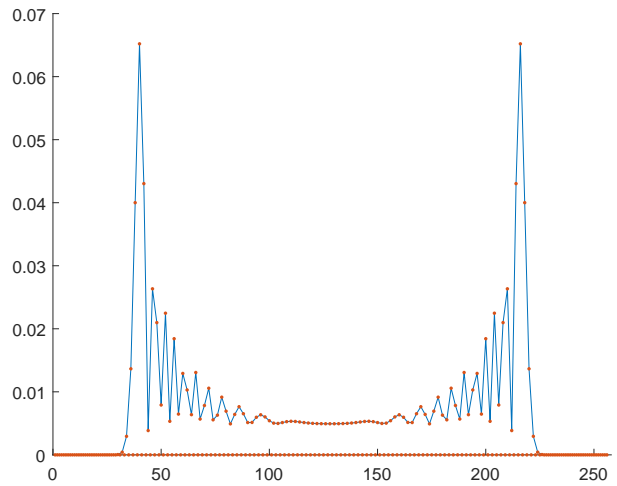


Figure 7. The simulation of quantum random walk with the initial state is $|01000000\rangle$ (128). The x axis represent the quantum state, from $|00000000\rangle$ (0) to $|11111111\rangle$ (255). The y axis represent the measurement probabilities (in the normalization units). The solid circles are the probabilities of each state. The statistical distribution can be observed by the line which linked by the nonzero circles.

$|x\rangle$ (x is a integer number) and the coin can be described with the basis states $|0\rangle$ and $|1\rangle$ [33, 34]. The evolutions of the walker and the coin are usually characterized by a time-independent unitary operator $U = TS_c|\phi\rangle$. In each step, the coin is tossed by

$$S_c(\phi) = \begin{pmatrix} \cos(\phi) & -\sin(\phi) \\ \sin(\phi) & \cos(\phi) \end{pmatrix}. \quad (15)$$

where ϕ is the rotation angle and equal to 45° in this work.

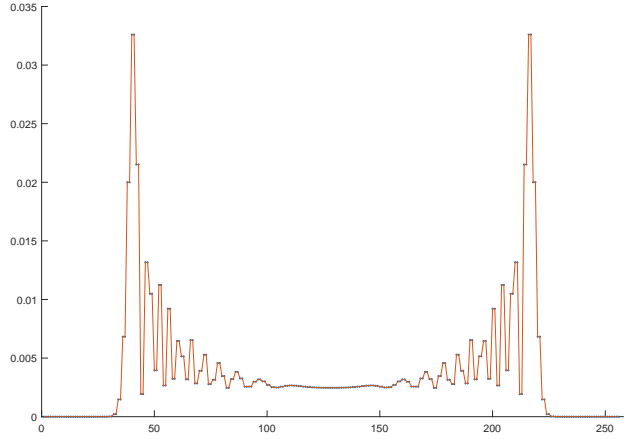


Figure 8. The simulation of quantum random walk with the initial state is $\frac{|01000000\rangle + |01000001\rangle}{2}$ (128,129). The x axis represent the quantum state, from $|00000000\rangle$ (0) to $|11111111\rangle$ (255). The y axis represent the measurement probabilities (in the normalization units). The solid circles are the probabilities of each state. The statistical distribution can be observed by the line which linked by all the circles.

The walker is shifted by $T = \Sigma|x+1\rangle\langle x| \otimes |1\rangle\langle 1| + \Sigma|x-1\rangle\langle x| \otimes |0\rangle\langle 0|$. In general, the result of the DTQWs with a

finite number of steps is determined by the initial states of the coin and the walker as well as the operator U . Obviously, the operator U can be realized by the algorithm we introduced above. The operator $|x+1\rangle\langle x|\otimes|1\rangle\langle 1|$ is the addition operator when the measurement of first auxiliary qubit is $|1\rangle$. Similarly the operator $|x-1\rangle\langle x|\otimes|0\rangle\langle 0|$ is the addition operator when the measurement of first auxiliary qubit is $|0\rangle$. So the first auxiliary qubit of our algorithm can be considered as the coin qubit of QRWs. Then we present two kinds of simulations with different initial state to demonstrate the QRWs by our algorithm. The size of the work system we choose is 8 and the auxiliary system is still a two-qubit system. The random walk step is 128 and that means we repeat the circuit in the Fig.1 for 128 times. The demonstration results with initial state $|01000000\rangle$ are shown in figure 7. We find that the probabilities of the odd state are all zero and only even state exists the probability of finding the particle. Moreover the statistical distribution has a good agreement with theory[34]. As we introduced before, our algorithm can be applied on the superposition state, so we choose another initial state $\frac{|01000000\rangle+|01000001\rangle}{\sqrt{2}}$, the simulation result is shown in Fig. 8. Obviously, now the odd state and even state are the same probabilities and the statistical distribution stay constant.

VI. CONLUSION

In summary, we propose a universal algorithm to realize addition and subtraction operator for the first time. In this algorithm addition and subtraction operators can be performed by the linear combination of unitary operations with a two-qubit ancillary system. Moreover, the number of ancillary qubits is independent with the size of work system. We implement this algorithm in a four-qubit NMR quantum processor. Since two qubits are the ancillary system, the size of work system is four (0,1,2,3). Without loss of generality, we choose two initial quantum state that one is the superposition state, the other is not. Our experimental results have shown good agreement with the theoretical predictions. Moreover, the application also proves that our algorithm is a universal method to realize addition and subtraction operators with a two-qubit ancillary system. They all prove that our algorithm can be a universal quantum control technology which can also be utilized in other quantum physical system such as NV center, superconducting, trapped ion and so on.

This work was supported by the National Basic Research Program of China (2015CB921002), the National Natural Science Foundation of China Grant Nos. (11175094, 91221205). Xiangyu Kong, Shijie Wei and Jingwei Wen are supported by the Fund of Key Laboratory (9140C75010215ZK65001).

[1] Sakurai J J, Tuan S F, Commins E D. Modern Quantum Mechanics, Revised Edition[J]. American Journal of Physics, 1995, 63(63):93-95.

[2] Borzov V V, Damaskinsky E V. Realization of the annihilation operator for generalized oscillator-like system by a differential operator[J]. 2001.

[3] Maalouf A I, Petersen I R. Coherent Control for a Class of Annihilation Operator Linear Quantum Systems[J]. IEEE Transactions on Automatic Control, 2011, 56(2):309-319.

[4] Parigi V, Zavatta A, Kim M, et al. Probing Quantum Commutation Rules by Addition and Subtraction of Single Photons to/from a Light Field[J]. Science, 2007, 317(5846):1890-1893.

[5] Urizar-Lanz I, Tóth G. Number-operator-annihilation-operator uncertainty as an alternative for the number-phase uncertainty relation[J]. Phys.rev.a, 2010, 81(5):90-90.

[6] Lundeen J S, Resch K J. Practical measurement of joint weak values and their connection to the annihilation operator[J]. Physics Letters A, 2005, 334(5):337-344.

[7] Hempel C, Maier C, Romero J, et al. Quantum chemistry calculations on a trapped-ion quantum simulator[J]. arXiv:1803.10238 [quant-ph]

[8] Mizrahi S S, Dodonov V V. Creating quanta with "annihilation" operator[J]. Journal of Physics A General Physics, 2012, 35(41):8847.

[9] Um, Mark, et al. "Phonon arithmetic in a trapped ion system." Nature communications 7 (2016): 11410.

[10] Bose, S. N. Plancks gesetz und lichtquantenhypothese. Z. Phys. 26, 178-181 (1924).

[11] Long G L 2006 Communications in Theoretical Physics 45(5) 825

[12] Gudder S 2007 Quantum Inf. Process. 6 37-48

[13] Wei S J, Ruan D, Long G L 2016 Sci. Rep. 6 30727

[14] Wei S J, Long G L. Duality quantum computer and the efficient quantum simulations[J]. Quantum Information Processing, 2016, 15(3): 1189-1212.

[15] L M K Vandersypen, I L Chuang, Reviews of modern physics 76(4): 1037 (2005).

[16] D. G. Cory, A. F. Fahmy and T. F. Havel, Proceedings of the National Academy of Sciences 94 1634-1639 (1997).

[17] D. Lu, N. Xu and R. Xu, Phys. Rev. Lett. 107 020501 (2011).

[18] Y. Lu, G. R. Feng, Y. S. Li, et al. Science bulletin 60 241-248 (2015).

[19] T. Xin, H. Li and B. X. Wang, Phys. Rev. A 92 022126 (2015).

[20] J. Pearson, G. R. Feng, C. Zheng, et al. Science China Physics 59 120312(2016).

[21] K. Li, G. Long and H. Katiyar, Phys. Rev. A, 95 022334 (2017).

[22] N. Khaneja, T. Reiss and C. Kehlet, Journal of magnetic resonance, 172 296-305 (2005).

[23] C. A. Ryan, C. Negrevergne and M. Laforest, Phys. Rev. A 78 012328 (2008).

[24] I. L. Chuang, L. M. K. Vandersypen and X. Zhou, Nature 393 143-146 (1998).

[25] I. L. Chuang, N. Gershenfeld and M. Kubinec, Phys. Rev. Lett. 80 3408 (1998).

[26] I. L. Chuang, N. Gershenfeld, M. G. Kubinec, et al. Physical and Engineering Sciences 454 447-467 (1998).

[27] Y. S. Weinstein, M. A. Pravia, E. M. Fortunato, S. Lloyd, and D. G. Cory, Phys. Rev. Lett. 86, 1889 (2001)

[28] Y. Aharonov, L. Davidovich, and N. Zagury, Quantum random walks, Phy. Rev. A 48, 1687 (1993).

[29] N. Shenvi, J. Kempe, and K. B. Whaley, Quantumrandom-walk search algorithm, Phys. Rev. A 67, 052307 (2003).

[30] A. Peruzzo, et al., Quantum walks of correlated photons, Science 329, 1500 (2010).

- [31] A. M. Childs, Universal computation by quantum walk, *Phys. Rev. Lett.* 102, 180501 (2009).
- [32] P. Kurzynski and A. Wojcik, Quantum walk as a generalized measuring device, *Phys. Rev. Lett.* 110, 200404(2013).
- [33] J. Kempe, Quantum random walks: an introductory overview, *Conte. Phys.* 44, 307 (2003).
- [34] S. E. Venegas-Andraca, Quantum walks: a comprehensive review, *Quan. Inf. Proc.* 11, 1015 (2012).